



Published in final edited form as:

*Ann Biomed Eng.* 2019 June ; 47(6): 1391–1399. doi:10.1007/s10439-019-02238-9.

## Optimizing accuracy of proximal femur elastic modulus equations

Asghar Rezaei<sup>1</sup>, Kent Carlson<sup>1</sup>, Hugo Giambini<sup>2</sup>, Samad Javid<sup>3</sup>, and Dan Dragomir-Daescu<sup>1</sup>

<sup>1</sup>Department of Physiology and Biomedical Engineering, Mayo Clinic, Rochester, MN

<sup>2</sup>Department of Biomedical Engineering, University of Texas at San Antonio, TX

<sup>3</sup>Division of Engineering, Mayo Clinic, Rochester, MN

### Abstract

Quantitative computed tomography-based finite element analysis (QCT/FEA) is a promising tool to predict femoral properties. One of the modeling parameters required as input for QCT/FEA is the elastic modulus, which varies with the location-dependent bone mineral density (ash density). The aim of this study was to develop optimized equations for the femoral elastic modulus. An inverse QCT/FEA method was employed, using an optimization process to minimize the error between the predicted femoral stiffness values and experimental values. We determined optimal coefficients of an elastic modulus equation that was a function of ash density only, and also optimal coefficients for several other equations that included along with ash density combinations of the variables sex and age. All of the optimized models were found to be more accurate than models from the literature. It was found that the addition of the variables sex and age to ash density made very minor improvements in stiffness predictions compared to the model with ash density alone. Even though the addition of age did not remarkably improve the statistical metrics, the effect of age was reflected in the elastic modulus equations as a decline of about 9% over a 60-year interval.

### Keywords

Optimization; mechanical testing; sex differences; femoral stiffness; inverse finite element analysis

## INTRODUCTION

Neck areal BMD measurement by Dual X-ray absorptiometry (DXA/aBMD) is the gold standard for the diagnosis of osteoporosis, and is also used to assess fracture risk.<sup>17</sup>

However, this method is two-dimensional (2D) and does not consider the complex geometry

---

**Corresponding Author:** Dan Dragomir-Daescu, Ph.D., Physiology and Biomedical Engineering, Mayo Clinic, 200 First Street, S.W., Rochester, MN 55905, United States, dragomirdaescu.dan@mayo.edu, Tel: 507-538-4946, Fax: 507-538-0038.

**Publisher's Disclaimer:** This Author Accepted Manuscript is a PDF file of an unedited peer-reviewed manuscript that has been accepted for publication but has not been copyedited or corrected. The official version of record that is published in the journal is kept up to date and so may therefore differ from this version.

### CONFLICT OF INTEREST

The authors declare that they have no conflict of interest.

of the bone. Therefore, previous studies have included femur geometry parameters along with DXA/BMD for hip structure analysis.<sup>1, 10</sup> DXA/aBMD also has been found to be sex-specific,<sup>10, 25, 28</sup> meaning that the same DXA/aBMD value, measured with clinical DXA scanners, leads to significantly smaller values of stiffness and strength in women compared to men. Although sex seems to be significant in addition to DXA/aBMD, previous studies found that the differences in geometry between women and men did not explain the sex dimorphism in femoral strength.<sup>28, 29</sup>

Quantitative computed tomography-based finite element analysis (QCT/FEA) is a tool that uses a more accurate representation of the 3D geometry and mineral distribution of the proximal femur to calculate femur properties. Many studies have shown QCT/FEA to be a better predictor of femoral properties than DXA/aBMD.<sup>3, 6, 13, 14, 19, 21, 23</sup> However, one of the main modeling parameters required as input for QCT/FEA is the elastic modulus equation of the bone,<sup>26, 31, 32</sup> which cannot be directly measured from mechanical testing. Several prior studies have focused on developing suitable mathematical equations between ash density and bone elastic modulus.<sup>15, 27</sup>

In a previous QCT/FEA study,<sup>29</sup> we used an ash density-elastic modulus relationship from the literature.<sup>24</sup> When comparing measured stiffness and strength values with corresponding QCT/FEA predictions, we found that age used as an independent variable was statistically significant, but that sex was insignificant. This indicates that QCT/FEA can account for differences in bones due to sex, but that it does not seem to fully account for differences due to age.

The aim of this study was to develop optimized ash density-elastic modulus equations for the proximal femur, in order to improve QCT/FEA estimation of femoral stiffness. Since our previous work indicated that QCT/FEA did not fully account for differences in bone due to age when age was considered independently as a variable, we included age here directly as a variable in the ash density-elastic modulus equation. We also included sex directly as a variable; although our prior results<sup>29</sup> using sex as an independent variable and using a published ash density-elastic modulus equation<sup>24</sup> indicated that QCT/FEA accounted well for differences in femoral stiffness due to sex, we were uncertain if this would remain true for other elastic modulus relationships.

## MATERIALS AND METHODS

While the femoral elastic modulus cannot be directly measured from mechanical testing outcomes due to the femur's complex geometry, the elastic modulus indirectly manifests itself in stiffness outcomes. Therefore, to assess the femoral elastic modulus, we obtained femoral stiffness values from a cohort of cadaveric proximal femurs that were mechanically tested to fracture. Then, an inverse QCT/FEA method was employed, using an optimization process to minimize the error between the measured and QCT/FEA-predicted femoral stiffness values. The inverse method used in this study optimizes the ash density-elastic modulus equation by minimizing the difference between the experimentally-measured and QCT/FEA-estimated stiffness values. This inverse method is similar to methods used in previous studies for material characterization.<sup>4, 11, 16</sup> This optimization process was repeated

for several proposed elastic modulus equations including variables to account for bone ash density distribution, sex and/or age. We also performed separate QCT/FEA analyses using previously published ash density-elastic modulus relationships, and compared their results with the outcomes of the current study.

### Experimental Approach

Sample preparation and mechanical testing protocols were described in detail previously,<sup>8,9</sup> and are summarized here for convenience. One hundred single fresh frozen human cadaveric proximal femurs were obtained after IRB approval. A statistical summary of the femoral data is shown in Table 1.

Femurs were screened using x-ray to rule out for metastatic disease or prior fracture, and then soft tissue was carefully removed. DXA/aBMD of each specimen was carefully measured in the neck region using a GE Lunar iDXA system (GE Healthcare Inc., Madison, WI). The femurs were cut to produce proximal femurs of length 255 mm (10 in.), and then the distal end of each femur was potted in an acrylic box that was used to mount the femur into the CT scanning and mechanical testing fixtures (see Figs. 1A and 1B). CT scanning was performed using a Siemens Somatom Definition Dual Source CT scanner (120 kVp, 216 mAs, 1 s rotation time, pitch = 1, slice thickness = 0.4 mm, and in-plane resolution = 0.3 mm–0.45 mm).<sup>9</sup>

The proximal femurs were mechanically tested to fracture in a sideways fall on the hip configuration.<sup>8</sup> The test speed was 100 mm/sec, which was found to be consistent with bone deformation due to a fall.<sup>12</sup> The force at the greater trochanter and the displacement at the femoral head were measured during fracture testing, and the slope of the linear portion of the force-displacement curve (from 20% to 80% of the measured yield force) was taken as the femoral stiffness.<sup>29</sup> Figure 1 shows the QCT scanning setup (Fig. 1A), the mechanical testing setup (Fig. 1B), and a force-displacement curve (Fig. 1C) from a cadaveric sample.

### QCT/FEA approach

The QCT/FEA technique included creating three-dimensional (3D) geometry from QCT imaging of each femur by segmentation, generating 3D finite element mesh, applying boundary conditions related to a sideways fall on the hip, and also assigning density and elastic modulus properties using the QCT Hounsfield units (HU).<sup>7</sup> From QCT imaging data, the bone surface was first generated in Mimics editing software (Materialise, Ann Arbor, MI), and then the 3D geometry was generated. A volume mesh was developed in this 3D geometry using an advancing front meshing method in ICEM CFD (ANSYS, Canonsburg PA). For each femur, the mesh contained between 600,000 and 800,000 elements. The mesh was generated using a protocol developed in a previous study, which was shown to produce converged results.<sup>7</sup> The volume mesh was imported into Mimics software again to assign an average HU value calculated from the QCT voxels to each finite element in the volume mesh. The range of HU values within a femur is expected to fall between about 0 and 3000 HU, so we created 300 bins, each with width 10 HUs. All values of HU < 0 were put into one additional bin, representing less dense materials like fat and marrow. The range of Hounsfield units covering the tissue domain was thus divided into 301 bins, approximating a

continuous distribution of grey scale values.<sup>29</sup> Ash density ( $\rho_{ash}$ ) for each element was calculated based on the HU values and the manufacturer's phantom calibration specifications (Mindways Inc., Austin TX). This resulted in a relationship of the form:<sup>5</sup>

$$\rho_{ash} = m \times HU + n, \quad (1)$$

where  $m$  and  $n$  were determined for each QCT scan using the known density of the rods in the calibration phantom. The isotropic elastic modulus ( $E$ ) for each material bin was calculated from  $\rho_{ash}$  based on different power law ash density-elastic modulus relations. Poisson's ratio was set to 0.3 for all materials. Each model was imported into ANSYS Mechanical APDL (ANSYS, Canonsburg PA), and a quasi-static analysis was performed using multi-point constraint (MPC) boundary conditions (BCs) to best match experimental testing BCs, including contact pressure distributions.<sup>30</sup> Force and displacement data were obtained for each QCT/FEA model to calculate femoral stiffness.<sup>7</sup>

### Femoral Ash Density-Elastic Modulus Relationships

Four different ash density-elastic modulus models, depending on bone density, sex, and/or age, were selected as listed in Table 2. For each model, all 100 samples were used simultaneously for optimization to estimate the unknowns of the model equations. Model 1 is the widely used ash density-elastic modulus equation with two unknown coefficients. Model 2 represents the effect of sex and density together in one model. Sex was directly included as a dummy variable ( $sex = 0$  for women and  $sex = 1$  for men). In Model 3, age was directly included in addition to density, to estimate the effect of age. The age-related decline was assumed to be linear above age 30 by using the term  $(age - 30)$ . There were no femurs in our cohort from ages less than 30 years old, so the term  $(age - 30)$  was never negative. Models 2 and 3 both resulted in three unknown coefficients to be determined. Model 4 consists of one equation directly including sex as a dummy variable as well as age in addition to density, resulting in an equation with four unknown coefficients.

### Inverse QCT/FEA Approach

Optimization procedures were used to determine the elastic properties of the femur; the ash density-elastic modulus equations described in the previous section were used sequentially for the elastic modulus in the FEA model to calculate the unknown coefficients. To this end, an objective function in the form of the root mean square (RMS) error was defined between experimentally measured stiffness ( $K_i$ ) and QCT/FEA-estimated stiffness ( $\hat{K}_i$ ) values as

$$J = \sqrt{\sum_{i=1}^n (K_i - \hat{K}_i)^2}, \quad (2)$$

where  $n = 100$  is the number of femurs used in the optimization process. The constants in the ash density-elastic modulus equations used in the QCT/FEA models were changed iteratively by the optimization algorithms to minimize the objective function. Using the optimization toolbox of MATLAB (MathWorks, Natick MA), the Nelder-Mead simplex

optimization algorithm,<sup>20</sup> a well-known simplex search algorithm (SSA) for finding a local minimum of multi-variable, unconstrained functions, was used to identify the unknown coefficients. When the change in the objective function for two consecutive iterations was less than an acceptable tolerance, the optimization process was stopped and the last set of material coefficients was reported as the optimal coefficients. This led to an optimal match between the QCT/FEA-estimated stiffness values and the experimental values. To ensure that the outcomes of the optimization process were unique and independent of the initial values, the optimization process was repeated with completely different initial values. Finally, several previously published bone ash density-elastic modulus relationships<sup>4, 11, 24</sup> were tested with our QCT/FEA models, and the QCT/FEA-estimated stiffness values using each of these models were also calculated and compared with the experimentally measured stiffness.

The number of iterations in each optimization varied from 67 for Model 1 to 327 for Model 4, totaling more than 96,000 QCT/FEA model simulations performed for this study.

### Statistical Analysis

Linear regression analyses were performed in JMP statistical software version 10.0.0 (SAS Institute Inc., Cary NC). These analyses were performed with experimentally measured stiffness as the dependent variable and QCT/FEA-estimated stiffness as the explanatory variable. Two adjusted coefficients of determination ( $R^2$  and  $\hat{R}^2$ ) were calculated; one with respect to the regression line representing the  $Y = mX + b$  ( $R^2$ ) representing the precision of the predictions; and the other with respect to  $Y = X(\hat{R}^2)$ , indicating the accuracy of the predictions. Also, concordance correlation coefficients (CCC) were estimated in MedCalc statistical software version 14.12.0 (MedCalc Software bvba, Ostend, Belgium) to analyze the agreement between QCT/FEA-predicted and experimentally-measured stiffness values. CCC was used to simultaneously measure the accuracy and precision of the QCT/FEA predictions for stiffness.<sup>22</sup>

## RESULTS

The optimization processes were performed and material model coefficients were determined for all proposed ash density-elastic modulus equations (Table 3). For each optimal equation, QCT/FEA stiffness values were calculated for all femurs in the cohort and compared for correlation with corresponding experimental values using the three different statistical performance metrics ( $R^2$ ,  $\hat{R}^2$ , and CCC values). For the models proposed in the current study,  $R^2$  values from regression lines ( $Y = mX + b$ ) varied very little, from 0.70 to 0.71, and  $\hat{R}^2$  values from the equation  $Y = X$  were all 0.63. The CCC values varied only slightly, from 0.83 to 0.84. Comparing Models 1 and 2, the three statistical measures remained essentially the same between the models, indicating that the incorporation of sex directly as a binary variable in the elastic modulus equation (Model 2) did not improve the performance of the equation to explain variations in the experimental stiffness. Compared with Model 1, the direct addition of age as a variable in Model 3 slightly improved the stiffness predictions by about 1% (for both  $R^2$  and CCC). When sex and age were included together with density (Model 4), the stiffness predictions were very similar to the ones from

Model 3 (with only density and age as variables), indicating that sex, again, did not add any extra information in Model 4 compared with Model 3.

For comparison, Table 3 also includes the results from QCT/FEA models run with each of three previously published material equations<sup>4, 11, 24</sup>. The  $R^2$  values from regression lines generated with the results of these models using ash density-elastic modulus equations from the literature varied from 0.66 to 0.72. The  $\hat{R}^2$  values from  $Y = X$  models generated with the results of these same models from previous studies were considerably smaller, ranging from -0.03 to 0.45. The corresponding CCC values were also smaller, ranging from 0.68 to 0.78.

Figure 2 illustrates elastic modulus variation with ash density for the different elastic modulus models. Model 1 is compared to Model 2 in Figure 2A, where Model 2 is shown as separate curves differentiated by sex. This plot illustrates that there is very little difference in these curves, which explains the statistical results in Table 3 that showed no improvement in performance between Model 1 and Model 2. The effect of age on the elastic properties of femurs is demonstrated in Figure 2B, by showing the elastic modulus curves for three different ages. Although adding age in Model 3 did not significantly improve the performance of QCT/FEA stiffness predictions for the entire cohort compared to Model 1 (see Table 3), the decline of the elastic modulus over 60 years of age (from age 30 to 90) was about 9% for a given ash density value (Fig. 2B). In Figure 2C, Model 3 and Model 4 are compared for a sixty-year-old to investigate the effect of sex on the elastic modulus of the proximal femurs when age is also included. The difference in sex was not distinguishable, which again is in agreement with the results in Table 3. Repeating this comparison at different ages produces analogously similar curves. Finally, in Figure 2D, the optimal Model 3 equation for a sixty-year-old is compared to the elastic modulus determined with ash density-elastic modulus equations from the literature.<sup>4, 11, 24</sup> This comparison shows that there is significant variation among these curves.

Next, the material models from Table 3 were used as the elastic properties of the femurs in our QCT/FEA models to estimate femoral stiffness, and their performance in terms of model precision and accuracy was assessed. The differences between precision, represented by  $R^2$  values (with respect to the line  $Y = mX + b$ ) obtained for each model, and accuracy, represented by  $\hat{R}^2$  values (with respect to the line  $Y = X$ ), are shown in Figure 3, which shows scatterplots of the measured and predicted stiffness values for four of the models considered in this study. Using elastic modulus Model 1 (Fig. 3A), the slope ( $m$ ) of the line  $Y = mX + b$  was 0.769, resulting in  $R^2 = 0.70$ , while the errors calculated with respect to the line  $Y = X$  yielded a value of  $\hat{R}^2 = 0.63$ . Using Model 4 (Fig. 3B), the slope of the line  $Y = mX + b$  increased to 0.816, indicating that the slope increased closer to a value of one, even though the  $R^2$  value increased only slightly going from Model 1 to Model 4, and the  $\hat{R}^2$  and CCC values of these two models were the same (Table 3).

Using the ash density-elastic modulus relation by Morgan et al.,<sup>24</sup> the QCT/FEA-estimated stiffness values explained 72% of the variability in experimental stiffness ( $R^2 = 0.72$ ) showing very good precision. The  $\hat{R}^2$  value resulting from this equation, on the other hand, was low ( $\hat{R}^2 = 0.35$ ), showing relatively weak accuracy. This is illustrated in Figure 3C,

where the regression line deviates significantly from the line  $Y = X$ , indicating that the stiffness of the stiffer femurs in our cohort were overestimated by the elastic modulus model from Morgan et al. Next, using the ash density-elastic modulus model from Eberle et al.,<sup>11</sup> our QCT/FEA method resulted in a wider cloud of data points around the regression line, leading to a lower  $R^2$  value of 0.66. Also, the majority of the data points were below the line  $Y = X$ , overestimating the experimental stiffness and leading to a negative  $\hat{R}^2$  value of  $-0.03$ , indicating poor accuracy (Fig. 3D).

## DISCUSSION

Using an inverse QCT/FEA technique for a cohort of 100 cadaveric proximal femurs, several forms of the ash density-elastic modulus equation were optimized with respect to experimentally-measured stiffness. Three statistical metrics were used to compare the performance of different material models to explain experimental stiffness. The first metric was the  $R^2$  value representing how close the predicted stiffness data points calculated using each elastic modulus model were to their regression line  $Y = mX + b$ , which is a measure of the elastic modulus model's precision, but not of its accuracy. The second metric was the  $\hat{R}^2$  value with respect to  $Y = X$ , which is a measure of the model's accuracy in producing a predicted stiffness that is in good agreement with the measured stiffness value. Note that a linear regression equation  $Y = mX + b$  that is significantly different from  $Y = X$ , regardless of how high the value of  $R^2$  is for that regression equation, indicates that the material model employed does not accurately represent the elastic modulus, underestimating or overestimating the elastic properties of the material. Also note that a model with high precision but not high accuracy may be sufficient if the quantity being predicted is the desired quantity, because the regression line can be used with the predicted value to estimate the true value. But since stiffness is modeled in an attempt to estimate femoral properties, accuracy is desired in addition to precision. Finally, the third metric, CCC, is a measure of both precision and accuracy between the predicted and measured stiffness values.<sup>22</sup>

The optimized models developed in the present study had precision values that were comparable to the most precise models from previous studies ( $R^2 \Rightarrow 0.70 - 0.71$  in the present models compared to 0.72 in the model from Morgan et al.<sup>24</sup>). More importantly, the present models were found to be much more accurate than any previously existing model  $\hat{R}^2 = 0.63$  in the present models compared to a maximum of 0.45 in the model from Cong et al.<sup>4</sup>).

As an example of the interpretation of these statistical metrics, consider the performance that resulted when we used the material equation from Eberle et al.<sup>11</sup> With this equation, the QCT/FEA-estimated stiffness values produced an acceptable  $R^2$  value of 0.66, indicating that this equation is precise enough to explain 66% of the variability in the femoral stiffness. However, the majority of the data points were below the line  $Y = X$  (see Fig. 3D), which is why the calculated  $\hat{R}^2$  is a negative value, indicating poor accuracy. It should be noted that Eberle et al. obtained their elastic modulus material equation from experimental data of femurs with a stance-like loading. This material equation, therefore, may not be accurate in explaining elastic properties of the proximal femur when undergoing a load in a sideways

fall on the hip, as in our current study. The QCT/FEA-estimated stiffness values using the material equation of Eberle et al. provided a CCC value of 0.68. This is a low value for CCC,<sup>22</sup> and therefore does not indicate good agreement between the prediction and the measurement.

The elastic modulus equation determines the accuracy of QCT/FEA-estimated femoral stiffness. Even though femoral stiffness is not a clinical measure of bone properties, it is a required quantity to estimate fracture strength using the QCT/FEA technique. Therefore, it is necessary to have an accurate elastic modulus in order to further accurately calculate fracture strength. The maximum  $\hat{R}^2$  value for femoral stiffness obtained in the current study was 0.63, which indicates that about 37% of the variability in femoral stiffness remains unexplained. This suggests the importance of contributing factors not considered in the present QCT/FEA approach such as bone microstructure, which cannot be fully captured by clinical CT scanners. Micro-CT analysis on trabecular and cortical bones could help explain more of the variability in experimental stiffness than clinical scanners, but they are impractical to use with patients.

One of the purposes of the current study was to provide more accurate ash density-elastic modulus equations using an inverse QCT/FEA approach with a relatively large sample size. Cong et al.<sup>4</sup> performed a similar approach to estimate the elastic modulus of proximal femurs, but with a smaller sample size of 22 femurs. Also, the QCT/FEA models created by Cong et al. used a direct boundary condition. In the current study, a MPC boundary condition was used instead, to more accurately mimic the experimental loading conditions.<sup>30</sup>

While the accuracy of stiffness predictions resulting from the elastic modulus equations of Morgan et al.<sup>24</sup> and Eberle et al.<sup>11</sup> were low for our entire cohort over a large range of BMD, these equations provided much more accurate stiffness predictions for low BMD values (Figs. 3C and 3D). Since femurs with lower stiffness values in our cohort mainly represent elderly women, the ash density-elastic modulus equations from Morgan et al.<sup>24</sup> and Eberle et al.<sup>11</sup> could be good estimates of the elastic properties of older women's femurs. This sub-population is more likely to be osteoporotic, and more vulnerable to falls and femoral fracture.

In our previous study,<sup>29</sup> which used the ash density-elastic modulus equation from Morgan et al.,<sup>24</sup> we found that QCT/FEA-estimated stiffness was insensitive to sex as an independent variable, which indicated that this technique can be used equally for women and men. In the current study, when sex was directly included in the elastic modulus equation (Model 2) that was optimized over the entire femur cohort (including both men and women), sex again did not improve the stiffness prediction, similar to our earlier findings.<sup>29</sup> The direct inclusion of age as a variable in the elastic modulus equations in the current study did not contribute considerably to precision or accuracy of the models. This can be seen by comparing the  $R^2$ ,  $\hat{R}^2$ , and CCC values of Models 1 and 3, and of Models 2 and 4, respectively. However, it is widely known that aging reduces bone density in both sexes.<sup>2, 18</sup> Even though the addition of age did not remarkably improve the statistical metrics in Models 3 and 4 compared to Models 1 and 2, respectively, the declining effect of age in the femoral elastic modulus was found to be about 9% for a given bone density value over a 60-year time interval. This

statistically insignificant reduction in the elastic modulus implies that bone fragility, a condition that increases bone fracture risk enhanced by reduction of bone mass and deterioration of microstructure in bone tissue,<sup>5</sup> may not be unambiguously associated to degradation of bone elastic modulus. Further studies should be performed to investigate this relation between bone fragility and bone material properties in order to understand the underlying mechanism of bone fracture in elderly populations.

Additionally, we did not take into account two important factors that could affect the macroscopic stiffness of the proximal femur: nonlinearity and anisotropy. Future studies should gather information on the intrinsic variance of the stiffness due to these two factors, in order to increase the predictive ability of QCT/FEA models for femoral stiffness.

In conclusion, based on our previous experimental femur fracture test results for a cohort of 100 cadaveric proximal femurs in a sideways fall-on-the-hip configuration, we derived optimized elastic modulus equations for our QCT/FEA model that result in more accurate femoral stiffness predictions, compared to QCT/FEA models that employ similar equations previously published in the literature. Statistical comparison of these new ash density-elastic modulus equations demonstrated that they implicitly account for sex and age.

## ACKNOWLEDGEMENTS

The study was financially supported by the Grainger Foundation: Grainger Innovation Fund. The CT imaging of the femurs was performed through the Opus CT Imaging Resource of Mayo Clinic (NIH construction grant RR018898). This publication was made possible by CTSA Grant Number UL1 TR000135 from the National Center for Advancing Translational Sciences (NCATS), a component of the National Institutes of Health (NIH). Also we would like to thank Timothy Rossman for his contribution to the optimization process.

## REFERENCE

1. Aldieri A, Terzini M, Osella G, Priola AM, Angeli A, Veltri A, Audenino AL and Bignardi C. Osteoporotic Hip Fracture Prediction: Is T-Score-Based Criterion Enough? A Hip Structural Analysis-Based Model. *Journal of biomechanical engineering* 140: 111004, 2018.
2. Anderson DE and Madigan ML. Effects of age-related differences in femoral loading and bone mineral density on strains in the proximal femur during controlled walking. *Journal of applied biomechanics* 29: 505–516, 2013. [PubMed: 23185080]
3. Cody DD, Gross GJ, Hou FJ, Spencer HJ, Goldstein SA and Fyhrie DP. Femoral strength is better predicted by finite element models than QCT and DXA. *Journal of biomechanics* 32: 1013–1020, 1999. [PubMed: 10476839]
4. Cong A, Buijs JO and Dragomir-Daescu D. In situ parameter identification of optimal density-elastic modulus relationships in subject-specific finite element models of the proximal femur. *Med Eng Phys* 33: 164–173, 2011. [PubMed: 21030287]
5. D'Elia G, Caracchini G, Cavalli L and Innocenti P. Bone fragility and imaging techniques. *Clinical Cases in mineral and bone metabolism* 6: 234, 2009. [PubMed: 22461252]
6. Dall'Ara E, Eastell R, Viceconti M, Pahr D and Yang L. Experimental Validation of DXA-based Finite Element models for prediction of femoral strength. *Journal of the Mechanical Behavior of Biomedical Materials* 2016.
7. Dragomir-Daescu D, Den Buijs JO, McEligot S, Dai Y, Entwistle RC, Salas C, Melton LJ, Bennet KE, Khosla S and Amin S. Robust QCT/FEA models of proximal femur stiffness and fracture load during a sideways fall on the hip. *Annals of Biomedical Engineering* 39: 742–755, 2011. [PubMed: 21052839]

8. Dragomir-Daescu D, Rezaei A, Rossman T, Uthamaraj S, Entwistle R, McEligot S, Lambert V, Giambini H, Jasiuk I and Yaszemski M. Method and Instrumented Fixture for Femoral Fracture Testing in a Sideways Fall-on-the-Hip Position. *Journal of visualized experiments: JoVE* 2017.
9. Dragomir-Daescu D, Rezaei A, Uthamaraj S, Rossman T, Bronk JT, Bolander M, Lambert V, McEligot S, Entwistle R and Giambini H. Proximal Cadaveric Femur Preparation for Fracture Strength Testing and Quantitative CT-based Finite Element Analysis. *JoVE (Journal of Visualized Experiments)* e54925–e54925, 2017.
10. Dragomir-Daescu D, Rossman TL, Rezaei A, Carlson KD, Kallmes DF, Skinner JA, Khosla S and Amin S. Factors associated with proximal femur fracture determined in a large cadaveric cohort. *Bone* 116: 196–202, 2018. [PubMed: 30096469]
11. Eberle S, Gottlinger M and Augat P. Individual density-elasticity relationships improve accuracy of subject-specific finite element models of human femurs. *J Biomech* 46: 2152–2157, 2013. [PubMed: 23895895]
12. Gilchrist S, Nishiyama K, De Bakker P, Guy P, Boyd S, Oxland T and Cripton P. Proximal femur elastic behaviour is the same in impact and constant displacement rate fall simulation. *Journal of biomechanics* 47: 3744–3749, 2014. [PubMed: 25443780]
13. Grassi L, Vaananen SP, Ristinmaa M, Jurvelin JS and Isaksson H. How accurately can subject-specific finite element models predict strains and strength of human femora? Investigation using full-field measurements. *J Biomech* 49: 802–806, 2016. [PubMed: 26944687]
14. Hambli R and Allaoui S. A robust 3D finite element simulation of human proximal femur progressive fracture under stance load with experimental validation. *Annals of Biomedical Engineering* 41: 2515–2527, 2013. [PubMed: 23864338]
15. Helgason B, Perilli E, Schileo E, Taddei F, Brynjólfsson S and Viceconti M. Mathematical relationships between bone density and mechanical properties: a literature review. *Clinical biomechanics* 23: 135–146, 2008. [PubMed: 17931759]
16. Huang H-L, Tsai M-T, Lin D-J, Chien C-S and Hsu J-T. A new method to evaluate the elastic modulus of cortical bone by using a combined computed tomography and finite element approach. *Computers in biology and medicine* 40: 464–468, 2010. [PubMed: 20304390]
17. Kanis JA Diagnosis of osteoporosis and assessment of fracture risk. *The Lancet* 359: 1929–1936, 2002.
18. Keaveny TM, Kopperdahl DL, Melton LJ, Hoffmann PF, Amin S, Riggs BL and Khosla S. Age-dependence of femoral strength in white women and men. *Journal of Bone and Mineral Research* 25: 994–1001, 2010. [PubMed: 19874201]
19. Keyak JH, Kaneko TS, Tehranzadeh J and Skinner HB. Predicting proximal femoral strength using structural engineering models. *Clinical orthopaedics and related research* 437: 219–228, 2005.
20. Klein K and Neira J. Nelder-mead simplex optimization routine for large-scale problems: A distributed memory implementation. *Computational Economics* 43: 447–461, 2014
21. Koivumäki JE, Thevenot J, Pulkkinen P, Kuhn V, Link TM, Eckstein F and Jämsä T. Ct-based finite element models can be used to estimate experimentally measured failure loads in the proximal femur. *Bone* 50: 824–829, 2012. [PubMed: 22306697]
22. Lin LI-K A concordance correlation evaluate reproducibility. *Biometrics* 255–268, 1989.
23. Mirzaei M, Keshavarzian M and Naeini V. Analysis of strength and failure pattern of human proximal femur using quantitative computed tomography (QCT)-based finite element method. *Bone* 64: 108–114, 2014 [PubMed: 24735974]
24. Morgan EF, Bayraktar HH and Keaveny TM. Trabecular bone modulus-density relationships depend on anatomic site. *Journal of biomechanics* 36: 897–904, 2003. [PubMed: 12757797]
25. Nasiri M and Luo Y. Study of sex differences in the association between hip fracture risk and body parameters by DXA-based biomechanical modeling. *Bone* 90: 90–98, 2016. [PubMed: 27292653]
26. Niebur GL, Feldstein MJ, Yuen JC, Chen TJ and Keaveny TM. High-resolution finite element models with tissue strength asymmetry accurately predict failure of trabecular bone. *Journal of biomechanics* 33: 1575–1583, 2000. [PubMed: 11006381]
27. Ramezanzadehkoldeh M and Skallerud BH. MicroCT-based finite element models as a tool for virtual testing of cortical bone. *Medical engineering & physics* 46: 12–20, 2017. [PubMed: 28528791]

28. Rezaei A and Dragomir-Daescu D. Femoral Strength Changes Faster With Age Than BMD in Both Women and Men: A Biomechanical Study. *Journal of Bone and Mineral Research* 30: 2200–2206, 2015. [PubMed: 26096829]
29. Rezaei A, Giambini H, Rossman T, Carlson KD, Yaszemski MJ, Lu L and Dragomir-Daescu D. Are DXA/aBMD and QCT/FEA Stiffness and Strength Estimates Sensitive to Sex and Age? *Annals of Biomedical Engineering* 1–10, 2017.
30. Rossman T, Kushvaha V and Dragomir-Daescu D. QCT/FEA predictions of femoral stiffness are strongly affected by boundary condition modeling. *Computer methods in biomechanics and biomedical engineering* 19: 208–216, 2016. [PubMed: 25804260]
31. Schileo E, Taddei F, Malandrino A, Cristofolini L and Viceconti M. Subject-specific finite element models can accurately predict strain levels in long bones. *Journal of biomechanics* 40: 2982–2989, 2007. [PubMed: 17434172]
32. van Rietbergen B, Weinans H, Huiskes R and Odgaard A. A new method to determine trabecular bone elastic properties and loading using micromechanical finite-element models. *Journal of biomechanics* 28: 69–81, 1995. [PubMed: 7852443]

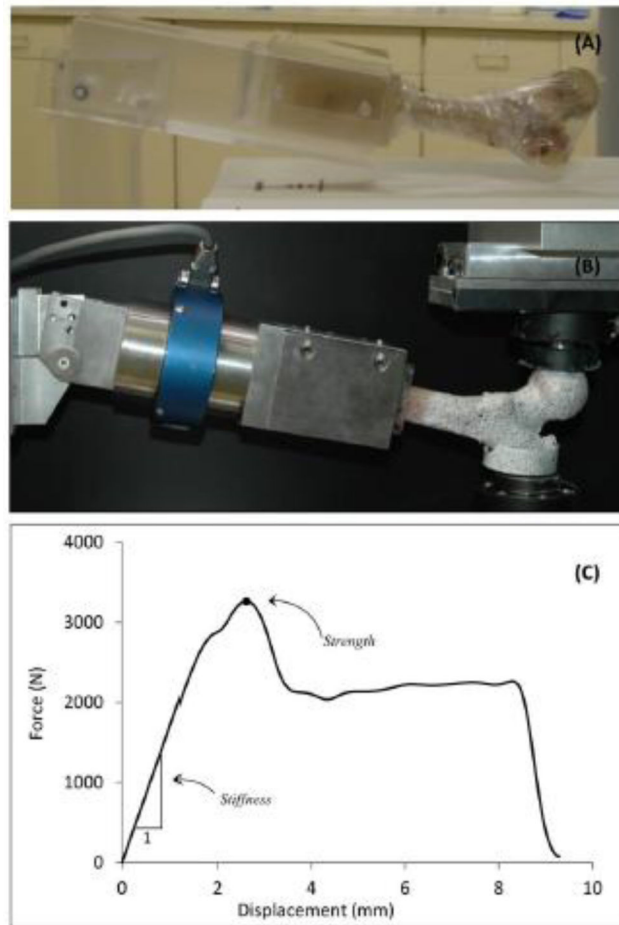


**Figure 1.**

(A) A cadaveric proximal femur held in the CT scanning fixture for imaging; (B) positioned in the mechanical testing fixture; and (C) a typical force-displacement curve displaying the linear region used to calculate femoral stiffness.

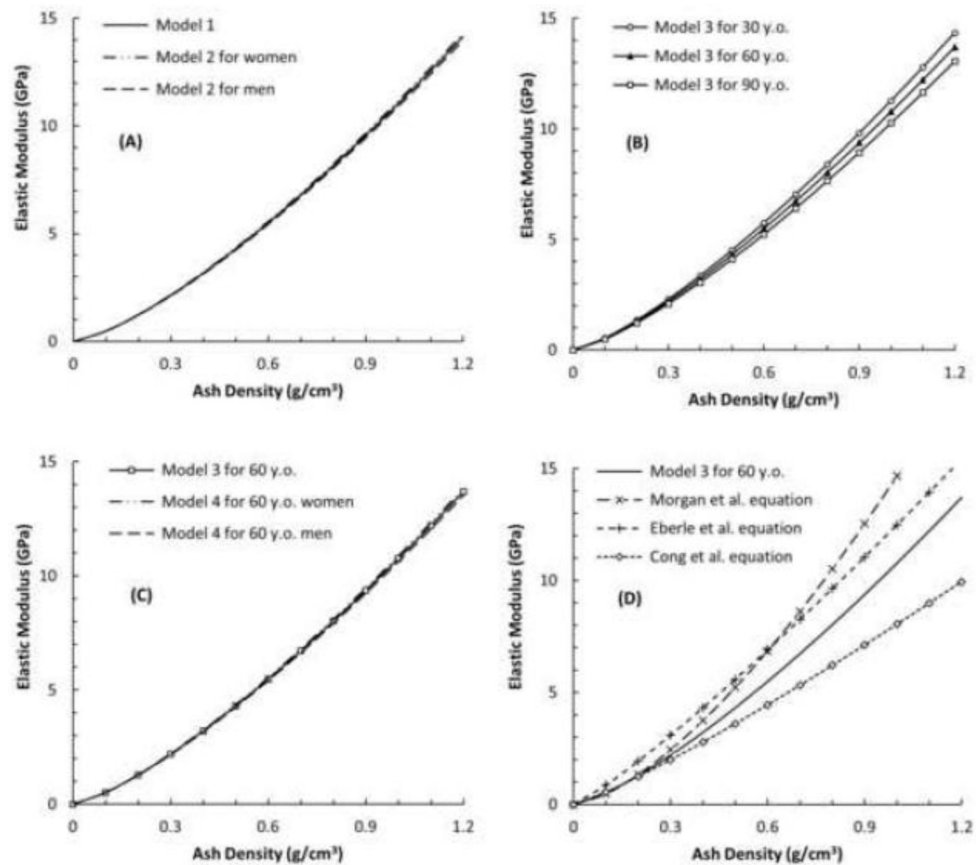


**Figure 2.**

Variation with density in elastic modulus equations: (A) comparing Models 1 and 2; (B) variation with age in Model 3, where curves representing three different ages (30, 60, and 90 years old) are provided to show how age negatively affects the elastic modulus; (C) comparing Models 3 and 4 at age 60 years old to see the effect of sex; and (D) comparing Model 3 (60 years old) and models from previous studies.<sup>4,11,24</sup>

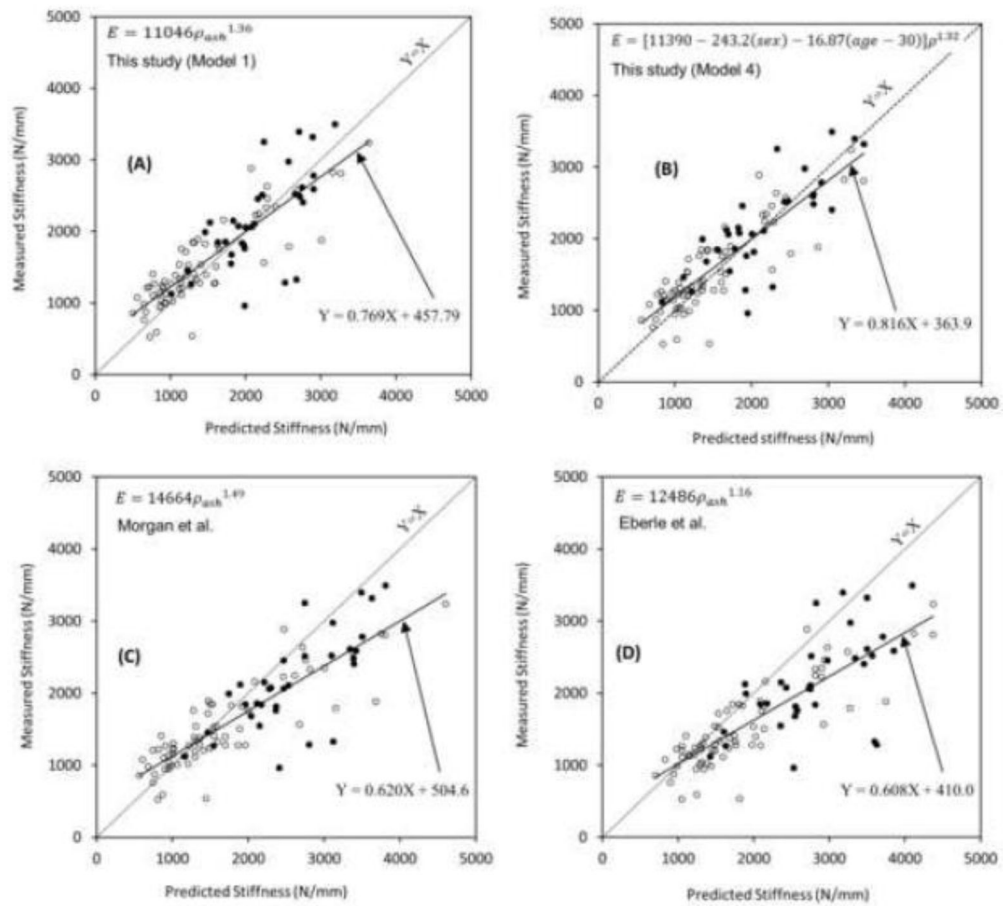


**Figure 3.** Measured stiffness vs predicted stiffness values when different ash density-elastic modulus equations are used; **(A)** Model 1; **(B)** Model 4; **(C)** equation proposed by Morgan et al.<sup>24</sup>; and **(D)** equation proposed by Eberle et al.<sup>11</sup> The solid and dashed lines in each scatterplot shows the regression and  $Y = X$  lines, respectively.

**Table 1.**Average ( $\pm$  standard deviation) values of BMD and age of the cadaveric cohort

	Women	Men	Entire Cohort
<b>No of Samples</b>	67	33	100
<b>Age (years)</b>	71.5 ( $\pm$ 14.1) [37-99]	66.7 ( $\pm$ 15.9) [34-91]	70 ( $\pm$ 15) [34-99]
<b>DXA/aBMD (g/cm<sup>2</sup>)</b>	0.722 ( $\pm$ 0.193)	0.894 ( $\pm$ 0.201)	0.779 ( $\pm$ 0.211)

Author Manuscript

Author Manuscript

Author Manuscript

Author Manuscript

**Table 2.**

Four different ash density-elastic modulus equations to model the elastic modulus of the proximal femur; the variable sex is assigned 0 and 1 for women and men, respectively.

Model	Equation	Unknown Coefficients
1	$E = a\rho_{ash}^b$	$a$ and $b$
2	$E = [a + d(\text{sex})]\rho^b$	$a$ , $b$ , and $d$
3	$E = [a + c(\text{age} - 30)]\rho^b$	$a$ , $b$ , and $c$
4	$E = [a + d(\text{sex}) + c(\text{age} - 30)]\rho^b$	$a$ , $b$ , $c$ , and $d$

**Table 3.**

Coefficients for the four proposed elastic modulus equations from the current study along with three previously-reported equations, as well as their performance in terms of the results from statistical analyses. The models from previous studies are abbreviated as M for Morgan et al.<sup>24</sup>, E for Eberle et al.<sup>11</sup>, and C for Cong et al.<sup>4</sup>

Model	Equations from current study	$R^2$	$\hat{R}^2$	ccc
1	$E = 11046\rho_{ash}^{1.36}$	0.70	0.63	0.83
2*	$E = [11161 - 252.2(\text{sex})]\rho^{1.36}$	0.70	0.63	0.83
3	$E = [11280 - 16.89(\text{age} - 30)]\rho_{ash}^{1.32}$	0.71	0.63	0.84
4*	$E = [11390 - 243.2(\text{sex}) - 16.87(\text{age} - 30)]\rho_{ash}^{1.32}$	0.71	0.63	0.84
<b>Equations from previous studies</b>				
M	$E = 14664\rho_{ash}^{1.49}$	0.72	0.35	0.78
E	$E = 12486\rho_{ash}^{1.16}$	0.66	-0.03	0.68
C	$E = 8050\rho_{ash}^{1.16}$	0.66	0.45	0.72

\* The variable *sex* is assigned 0 for women and 1 for men cohort.